

Emergent second law for non-equilibrium steady states

Nahuel Freitas¹ and Massimiliano Esposito¹

¹*Complex Systems and Statistical Mechanics, Department of Physics and Materials Science,
University of Luxembourg, L-1511 Luxembourg, Luxembourg*

(Dated: January 25, 2022)

The Gibbs distribution universally characterizes states of thermal equilibrium. In order to extend the Gibbs distribution to non-equilibrium steady states, one must relate the self-information $\mathcal{I}(x) = -\log(P_{\text{ss}}(x))$ of microstate x to measurable physical quantities. This is a central problem in non-equilibrium statistical physics. By considering open systems described by stochastic dynamics which become deterministic in the macroscopic limit, we show that changes $\Delta\mathcal{I} = \mathcal{I}(x_t) - \mathcal{I}(x_0)$ in steady state self-information along deterministic trajectories can be bounded by the macroscopic entropy production Σ . This bound takes the form of an emergent second law $\Sigma + k_b\Delta\mathcal{I} \geq 0$, which contains the usual second law $\Sigma \geq 0$ as a corollary, and is saturated in the linear regime close to equilibrium. In summary, we obtain a tighter version of the second law of thermodynamics that provides a link between the deterministic relaxation of a system and the non-equilibrium fluctuations at steady state.

PACS numbers:

I. INTRODUCTION

When a system is at equilibrium with its environment (i.e., when no energy currents are exchanged) the probability of a given microstate \mathbf{x} is given by the Gibbs distribution [1–3]

$$P_{\text{eq}}(\mathbf{x}) = e^{-\beta\Phi(\mathbf{x})}/Z, \quad (1)$$

where $\beta = (k_bT)^{-1}$ is the inverse temperature of the environment, $\Phi(\mathbf{x})$ is the free energy of microstate \mathbf{x} (for states with no internal entropy, $\Phi(\mathbf{x})$ is just the energy), and $Z = \sum_{\mathbf{x}} \exp(-\beta\Phi(\mathbf{x}))$ is the partition function. This central result of equilibrium statistical physics has universal validity and its relevance in most areas of physics cannot be overstated. A natural question is whether or not a similar result also holds for non-equilibrium steady states (NESSs), when the system is maintained out of thermal equilibrium by external drives and subjected to constant flows of energy. In this case, one can always write the steady state distribution over microstates as

$$P_{\text{ss}}(\mathbf{x}) = e^{-\mathcal{I}(\mathbf{x})} \quad (2)$$

in terms of the *self-information* $\mathcal{I}(\mathbf{x})$, also known as fluctuating entropy [4]. In order to provide a useful generalization of the Gibbs distribution to NESSs one must relate the self-information $\mathcal{I}(x)$ to measurable physical quantities. This quest has a long history, starting with the seminal contributions of Lebowitz and MacLennan [5–7] and followed by other works [8–14]. However, it still remains an open problem in non-equilibrium statistical physics, since previous formal results are simply not practical in computations, due to the fact that they involve averages over stochastic trajectories.

In this article we prove, for a very general class of open systems displaying a macroscopic limit where a deterministic dynamics emerges, the following fundamental bound on changes of self-information:

$$\Sigma_a \equiv \Sigma + k_b(\mathcal{I}(\mathbf{x}_t) - \mathcal{I}(\mathbf{x}_0)) \geq 0, \quad (3)$$

where Σ is the entropy production along a *deterministic trajectory* from microstate \mathbf{x}_0 to microstate \mathbf{x}_t . To arrive at Eq. (3), we consider stochastic systems with a well defined macroscopic limit. For example, the concentrations $\mathbf{x} = (x_1, x_2, \dots)$ of different chemical species reacting in a solution are stochastic quantities, and their evolution is therefore described by a probability distribution $P_t(\mathbf{x})$ at time t . However, as the volume V of the solution is increased, the distribution $P_t(\mathbf{x})$ becomes strongly localised around the most probable values \mathbf{x}_t for the concentrations at time t . The values \mathbf{x}_t follow a deterministic dynamics that is in general non-linear. An analogous situation is encountered in electronic circuits, where the state variables \mathbf{x} are now the electric charge at the nodes of a circuit, and the macroscopic limit corresponds to increasing the typical capacitance C of the nodes (as well as the conductivity of the conduction channels connecting pairs of nodes). The remarkable feature of the result in Eq. (3) is that it provides a link between the deterministic dynamics that emerges in the macroscopic limit and the fluctuations observed at steady state. For example, in an electronic circuit powered by voltage sources and working at temperature T , the entropy production is given by $T\Sigma = -\int_0^t \dot{Q}(\mathbf{x}_{t'}) dt'$, where $-\dot{Q}$ is the rate of heat dissipation in the conductive elements of the circuit, and can be easily evaluated for a deterministic trajectory initialized in state \mathbf{x}_0 and ending at \mathbf{x}_t . Then, by Eq. (3), the quantity $-\Sigma/k_b$ provides a lower bound to the change of steady state self-information $\mathcal{I}(\mathbf{x}_t) - \mathcal{I}(\mathbf{x}_0)$ along the trajectory.

We interpret our result as an emergent second law of thermodynamics, that is stronger than the usual second law $\Sigma \geq 0$. This last inequality is recovered from Eq. (3) by considering the fact that $\Delta\mathcal{I} = \mathcal{I}(\mathbf{x}_t) - \mathcal{I}(\mathbf{x}_0) \leq 0$ (the steady state self-information is a Lyapunov function of the deterministic dynamics [15]). In addition to its conceptual value, our result offers a practical tool to approximate or bound non-equilibrium distributions, that

can typically only be accessed via stochastic numerical methods (for example the Gillespie algorithm). In contrast, Eq. (3) only requires to know the deterministic dynamics of the system, which is directly given by the well known network analysis techniques commonly applied in electronic circuits and chemical reaction networks. Furthermore, the inequality in Eq. (3) is saturated close to equilibrium, leading to a powerful linear response theory [30]. Explicitly, to first order in the driving taking the system out of equilibrium, we can write:

$$\begin{aligned} \mathcal{I}(\mathbf{x}_t) - \mathcal{I}(\mathbf{x}_0) &\simeq -\Sigma/k_b & (4) \\ &= \beta \left[\Phi(\mathbf{x}_t) - \Phi(\mathbf{x}_0) - \int_0^t dt' \dot{W}(\mathbf{x}_{t'}) \right], \end{aligned}$$

where \dot{W} is the rate of work performed on the system by external sources. From Eq. (4), we see that if $\dot{W} = 0$ we recover, up to an irrelevant constant, $\mathcal{I}(\mathbf{x}) = \beta\Phi(\mathbf{x})$, in accordance to the Gibbs distribution in Eq. (1). As an example, we apply Eqs. (3) and (4) to a realistic model of non-equilibrium electronic memory: the normal implementation of SRAM (static random access memory) cells in CMOS (complementary metal-oxide-semiconductor) technology. These memories have a non-equilibrium phase transition from a monostable phase to a bistable phase that allows the storage of a bit of information. As we will see, the transition is well captured by Eq. (4), while Eq. (3) allows to bound the probability of fluctuations around the deterministic fixed points.

II. BASIC SETUP

To obtain Eq. (3) we consider stochastic systems described by autonomous Markov jump processes. Thus, let $\{\mathbf{n} \in \mathbb{N}^k\}$ be the set of possible states of the system, and $\lambda_\rho(\mathbf{n})$ be the rates at which jumps $\mathbf{n} \rightarrow \mathbf{n} + \Delta_\rho$ occur, for $\rho = \pm 1, \pm 2, \dots$ and $\Delta_{-\rho} = -\Delta_\rho$. Each state has energy $E(\mathbf{n})$ and internal entropy $S(\mathbf{n})$. Thermodynamic consistency is introduced by the *local detailed balance* (LDB) condition [16, 17]. It relates the forward and backward jump rates of a given transition with the associated entropy production:

$$\sigma_\rho = \log \frac{\lambda_\rho(\mathbf{n})}{\lambda_{-\rho}(\mathbf{n} + \Delta_\rho)} = -\beta [\Phi(\mathbf{n} + \Delta_\rho) - \Phi(\mathbf{n}) - W_\rho(\mathbf{n})]. \quad (5)$$

In the previous equation, $\Phi(\mathbf{n}) = E(\mathbf{n}) - TS(\mathbf{n})$ is the free energy of state \mathbf{n} , and $W_\rho(\mathbf{n})$ is the non-conservative work provided by external sources during the transition. For simplicity, we have considered isothermal conditions at inverse temperature $\beta = (k_b T)^{-1}$, and therefore the system is taken away from equilibrium by the external work sources alone. More general situations in which a system interacts with several reservoirs at different temperatures can be treated in the same way, this time in terms of a Massieu potential taking the place of $\beta\Phi(\mathbf{n})$ [16]. Important classes of systems accepting the previous description are chemical reaction

networks and electronic circuits, which are powered by chemical or electrostatic potential differences, respectively. Note that, by energy conservation, the heat provided by the environment during transition $\mathbf{n} \rightarrow \mathbf{n} + \Delta_\rho$ is $Q_\rho(\mathbf{n}) = E(\mathbf{n} + \Delta_\rho) - E(\mathbf{n}) - W_\rho(\mathbf{n})$, and therefore $k_b \sigma_\rho = -Q_\rho(\mathbf{n})/T + S(\mathbf{n} + \Delta_\rho) - S(\mathbf{n})$.

The probability distribution $P_t(\mathbf{n})$ over the states of the system at time t evolves according to the master equation

$$\partial_t P_t(\mathbf{n}) = \sum_\rho [\lambda_\rho(\mathbf{n} - \Delta_\rho) P_t(\mathbf{n} - \Delta_\rho) - \lambda_\rho(\mathbf{n}) P_t(\mathbf{n})]. \quad (6)$$

From the master equation and the LDB conditions one can derive the energy balance

$$d_t \langle E \rangle = \langle \dot{W} \rangle + \langle \dot{Q} \rangle, \quad (7)$$

and the usual version of the second law:

$$\dot{\Sigma} = \dot{\Sigma}_e + d_t \langle S \rangle \geq 0. \quad (8)$$

In the previous equations, $\langle S \rangle = \sum_{\mathbf{n}} P_t(\mathbf{n}) (S(\mathbf{n}) - k_b \log(P_t(\mathbf{n})))$ is the entropy of the system, $\langle E \rangle = \sum_{\mathbf{n}} E(\mathbf{n}) P_t(\mathbf{n})$ is the average energy, and $\dot{\Sigma}_e$ is the entropy flow rate, given by

$$T \dot{\Sigma}_e = -\langle \dot{Q} \rangle = -\sum_{\rho, \mathbf{n}} Q_\rho(\mathbf{n}) j_\rho(\mathbf{n}) \quad (9)$$

where we also defined the heat rate $\langle \dot{Q} \rangle$ in terms of the probability currents $j_\rho(\mathbf{n}) = \lambda_\rho(\mathbf{n}) P_t(\mathbf{n})$ (the work rate $\langle \dot{W} \rangle$ is analogously defined as $\langle \dot{W} \rangle = \sum_{\rho, \mathbf{n}} W_\rho(\mathbf{n}) j_\rho(\mathbf{n})$). Finally, Eq. (8) can be also expressed as:

$$T \dot{\Sigma} = -d_t \langle F \rangle + \langle \dot{W} \rangle \geq 0 \quad (10)$$

where $\langle F \rangle = \langle E \rangle - T \langle S \rangle$ is the non-equilibrium free energy.

Adiabatic/non-adiabatic decomposition – If the support of $P_t(\mathbf{n})$ can be restricted to a finite subspace of the state space, the Perron-Frobenius theorem states that the master equation in Eq. (6) has a unique steady state $P_{ss}(\mathbf{n})$. Once the steady state is attained, the entropy production rate $\dot{\Sigma}$ matches the entropy flow rate $\dot{\Sigma}_e$. An interesting decomposition of the entropy production rate can be obtained by considering the relative entropy $D = \sum_{\mathbf{n}} P_t(\mathbf{n}) \log(P_t(\mathbf{n})/P_{ss}(\mathbf{n}))$ between the instantaneous distribution $P_t(\mathbf{n})$ and the steady state distribution $P_{ss}(\mathbf{n})$. Then, it is possible to show that $\dot{\Sigma} = \dot{\Sigma}_a + \dot{\Sigma}_{na}$, where

$$\dot{\Sigma}_a = \frac{k_b}{2} \sum_{\rho, \mathbf{n}} (j_\rho(\mathbf{n}) - j_{-\rho}(\mathbf{n} + \Delta_\rho)) \log \frac{j_\rho^{ss}(\mathbf{n})}{j_{-\rho}^{ss}(\mathbf{n} + \Delta_\rho)}, \quad (11)$$

and

$$\begin{aligned} \dot{\Sigma}_{na} &= \frac{k_b}{2} \sum_{\rho, \mathbf{n}} (j_\rho(\mathbf{n}) - j_{-\rho}(\mathbf{n} + \Delta_\rho)) \log \frac{P_t(\mathbf{n}) P_{ss}(\mathbf{n} + \Delta_\rho)}{P_{ss}(\mathbf{n}) P_t(\mathbf{n} + \Delta_\rho)} \\ &= -k_b d_t D \end{aligned} \quad (12)$$

are the *adiabatic* and *non-adiabatic* contributions to the entropy production rate $\dot{\Sigma}$, respectively. In Eq. (11) we have introduced the steady state probability currents $j_\rho^{\text{ss}}(\mathbf{n}) = \lambda_\rho(\mathbf{n})P_{\text{ss}}(\mathbf{n})$. The non-adiabatic contribution $\dot{\Sigma}_{\text{na}}$ is related to the relaxation of the system towards the steady state, since it vanishes when the steady state is reached. This is further evidenced by the identity in the second line of Eq. (12): a reduction in the relative entropy between $P_t(\mathbf{n})$ and $P_{\text{ss}}(\mathbf{n})$ leads to a positive non-adiabatic entropy production. The adiabatic contribution $\dot{\Sigma}_{\text{a}}$ corresponds to the dissipation of ‘housekeeping heat’ [19, 20], and at steady state matches the entropy flow rate $\dot{\Sigma}_{\text{e}}$. An important property of the previous decomposition is that both contributions are individually positive: $\dot{\Sigma}_{\text{a}} \geq 0$ and $\dot{\Sigma}_{\text{na}} \geq 0$ [21–24]. Thus, the last inequality and the second line in Eq. (12) imply that the relative entropy D decreases monotonically, and since D is positive by definition, it is a Lyapunov function for the stochastic dynamics.

Macroscopic limit – In the following we will assume the existence of a scale parameter Ω controlling the size of the system in question. For example, Ω can be taken to be the volume V of the solution in well-mixed chemical reaction networks, or the typical value C of capacitance in the case of electronic circuits (see the example below). In addition, we will assume that for large Ω i) the transition rates $\lambda_\rho(\mathbf{n})$ are proportional to Ω , ii) that the typical values of the density $\mathbf{x} = \mathbf{n}/\Omega$ are intensive, and iii) that the internal energy and entropy functions $E(\mathbf{n})$ and $S(\mathbf{n})$ are extensive. Under those conditions, the probability distribution $P_t(\mathbf{x})$ satisfies a large deviations (LD) principle [26–28]:

$$P_t(\mathbf{x}) \asymp e^{-\Omega I_t(\mathbf{x})}, \quad (13)$$

where $I_t(\mathbf{x})$ is a positive, time-dependent rate function. Indeed, plugging the previous ansatz in the master equation of Eq. (6) and keeping only the dominant terms in $\Omega \rightarrow \infty$, we see that $I_t(\mathbf{x})$ evolves according to

$$\partial_t I_t(\mathbf{x}) = \sum_\rho \omega_\rho(\mathbf{x}) \left[1 - e^{\Delta_\rho \cdot \nabla I_t(\mathbf{x})} \right], \quad (14)$$

where $\omega_\rho(\mathbf{x}) = \lim_{\Omega \rightarrow \infty} \lambda_\rho(\Omega \mathbf{x})/\Omega$ are the scaled jump rates [25, 28]. Also, in the macroscopic limit the LDB conditions in Eq. (5) take the form

$$\log \frac{\omega_\rho(\mathbf{x})}{\omega_{-\rho}(\mathbf{x})} = -\beta [\Delta_\rho \cdot \nabla \phi(\mathbf{x}) - W_\rho(\mathbf{x})], \quad (15)$$

in terms of the free energy density $\phi(\mathbf{x}) = \lim_{\Omega \rightarrow \infty} \Phi(\Omega \mathbf{x})/\Omega$ (internal energy and entropy densities $\epsilon(\mathbf{x})$ and $s(\mathbf{x})$ satisfying $\phi(\mathbf{x}) = \epsilon(\mathbf{x}) - Ts(\mathbf{x})$ can be defined in the same way). From Eq. (13) we see that as Ω is increased, $P_t(\mathbf{x})$ is increasingly localised around the minimum of the rate function $I_t(\mathbf{x})$, which is the most probable value. Also, deviations from that typical state are exponentially suppressed in Ω . Thus, the limit

$\Omega \rightarrow \infty$ is a macroscopic low-noise limit where a deterministic dynamic emerges. In fact, from Eq. (14) one can show that the evolution of the minima \mathbf{x}_t of $I_t(\mathbf{x})$ is ruled by the closed non-linear differential equations

$$d_t \mathbf{x}_t = \mathbf{u}(\mathbf{x}_t) \quad \text{with} \quad \mathbf{u}(\mathbf{x}) = \sum_{\rho > 0} i_\rho(\mathbf{x}) \Delta_\rho, \quad (16)$$

where $i_\rho(\mathbf{x}) = \omega_\rho(\mathbf{x}) - \omega_{-\rho}(\mathbf{x})$ are the scaled deterministic currents [28]. The vector field $\mathbf{u}(\mathbf{x})$ corresponds to the deterministic drift in state space. For chemical reaction networks the dynamical equations in Eq. (16) are the chemical rate equations, while for electronic circuits they are provided by regular circuit analysis.

In the following section we obtain bounds for the steady state rate function $I_{\text{ss}}(\mathbf{x})$, that according to Eq. (14) satisfies:

$$0 = \sum_\rho \omega_\rho(\mathbf{x}) \left[1 - e^{\Delta_\rho \cdot \nabla I_{\text{ss}}(\mathbf{x})} \right]. \quad (17)$$

Note that, by Eq. (13), the steady state self-information introduced in Eq. (2) satisfies $\mathcal{I}(\mathbf{x}) = \Omega I_{\text{ss}}(\mathbf{x})$ to dominant order in the macroscopic limit.

III. EMERGENT SECOND LAW

The positivity of the adiabatic and non-adiabatic contributions to the entropy production, $\dot{\Sigma}_{\text{a}} \geq 0$ and $\dot{\Sigma}_{\text{na}} \geq 0$, in addition to the usual second law $\dot{\Sigma} \geq 0$, have been called the ‘three faces of the second law’ [22]. In [25], the inequality $\dot{\Sigma}_{\text{na}} = -k_b d_t D \geq 0$ was put forward as an ‘emergent’ second law. There, $\mathcal{F} = k_b D$ was interpreted as an alternative non-equilibrium free energy, with a balance equation $d_t \mathcal{F} = \dot{\Sigma}_{\text{a}} - \dot{\Sigma} \leq 0$ (note the analogy with Eq. (10)). Then, the adiabatic contribution $\dot{\Sigma}_{\text{a}}$ was interpreted as an energy input, which at steady state balances the dissipation $\dot{\Sigma}$. Although this point of view is compelling, it is hindered by the fact that there is no clear interpretation of $\dot{\Sigma}_{\text{a}}$ away from the steady state, that would allow to compute this quantity in terms of actual physical currents. In this work we take the other possible road, and investigate the interpretation and consequences of $\dot{\Sigma}_{\text{a}} \geq 0$. We begin by rewriting Eq. (11) using the LDB conditions of Eq. (5) and the definition of \mathcal{I} in Eq. (2), obtaining:

$$\dot{\Sigma}_{\text{a}} = \dot{\Sigma} + k_b d_t \langle \mathcal{I} \rangle \geq 0, \quad (18)$$

where we have defined $\langle \mathcal{I} \rangle = \sum_{\mathbf{n}} \mathcal{I}(\mathbf{n}) P_t(\mathbf{n})$ as the average of the steady state self-information $\mathcal{I}(\mathbf{n}) = -\log(P_{\text{ss}}(\mathbf{n}))$, computed over the instantaneous distribution. Eq. (18) has been already obtained in [21–23], although it was not explicitly written in terms of the self-information \mathcal{I} . Thus, changes in average self-information can be bounded by the entropy production, that can in turn be computed or measured in terms of actual energy and entropy flows (see Eqs. (8) and (9)). However, the

result in Eq. (18) is not yet in an useful form, since the average $\langle \mathcal{I} \rangle$ does not depend only on $\mathcal{I}(\mathbf{n})$, the unknown quantity we are interested in, but also on the instantaneous distribution $P_t(\mathbf{n})$, that is also typically unknown. This issue is circumvented in the macroscopic limit, since in that case $P_t(\mathbf{x})$ is strongly localised around the deterministic values \mathbf{x}_t , and therefore $\langle \mathcal{I} \rangle \simeq \Omega I_{\text{ss}}(\mathbf{x}_t)$ to dominant order in $\Omega \rightarrow \infty$. Thus, in the same limit, Eq. (11) for the adiabatic entropy production rate $\dot{\Sigma}_a$ reduces to

$$\dot{\Sigma}_a/\Omega = \dot{\Sigma}/\Omega + k_b d_t I_{\text{ss}}(\mathbf{x}_t) \geq 0. \quad (19)$$

Our central result in Eq. (3) is obtained by integrating Eq. (19) along deterministic trajectories (satisfying Eq. (16)). It is also useful to write down the first and second laws in the macroscopic limit. The energy balance in Eq. (7) reduces to

$$d_t \epsilon(\mathbf{x}_t) = \mathbf{u}(\mathbf{x}_t) \cdot \nabla \epsilon(\mathbf{x}_t) = \dot{w}(\mathbf{x}_t) + \dot{q}(\mathbf{x}_t), \quad (20)$$

where the scaled heat and work rates for state \mathbf{x} are defined as $\dot{q}(\mathbf{x}) = \sum_{\rho>0} i_\rho(\mathbf{x}) Q_\rho(\mathbf{x})$ and $\dot{w}(\mathbf{x}) = \sum_{\rho>0} i_\rho(\mathbf{x}) W_\rho(\mathbf{x})$, respectively. Finally, while the entropy flow rate $\dot{\Sigma}_e = -\Omega \dot{q}(\mathbf{x}_t)/T$ is extensive, the Shannon contribution $S_{\text{sh}} = -\sum_{\mathbf{n}} P_t(\mathbf{n}) \log(P_t(\mathbf{n}))$ to the internal entropy is sub-extensive in Ω . Therefore, the second law in Eq. (8) reduces to

$$\dot{\Sigma}/\Omega = -\dot{q}(\mathbf{x}_t)/T + d_t s(\mathbf{x}_t) \geq 0. \quad (21)$$

Linear response regime – We will now show that to first order in the work contributions $W_\rho(\mathbf{x})$ the inequality in Eq. (19) is saturated. In first place we rewrite Eq. (19) as

$$\dot{\Sigma}_a/(k_b \Omega) = \mathbf{u}(\mathbf{x}_t) \cdot \nabla (I_{\text{ss}}(\mathbf{x}) - \beta \phi(\mathbf{x}))|_{\mathbf{x}=\mathbf{x}_t} + \beta \dot{w}(\mathbf{x}_t). \quad (22)$$

Also, we note that in detailed balanced settings (i.e., if $W_\rho(\mathbf{x}) = 0 \forall \rho, \mathbf{x}$) the steady state rate function is just $I_{\text{ss}}(\mathbf{x}) = \beta \phi(\mathbf{x})$, in accordance to the Gibbs distribution (this follows from Eqs. (15) and (17)). Thus, the difference $g(\mathbf{x}) \equiv I_{\text{ss}}(\mathbf{x}) - \beta \phi(\mathbf{x})$ appearing in Eq. (19) quantifies the deviations from thermal equilibrium. Expanding Eq. (17) to first order in $W_\rho(\mathbf{x})$ and $g(\mathbf{x})$, it can be shown that

$$\mathbf{u}^{(0)}(\mathbf{x}) \cdot \nabla g(\mathbf{x}) = -\beta \dot{w}^{(0)}(\mathbf{x}) + \mathcal{O}(W_\rho^2), \quad (23)$$

where $\mathbf{u}^{(0)}(\mathbf{x}) = \sum_{\rho>0} i_\rho^{(0)}(\mathbf{x}) \Delta_\rho$ and $\dot{w}^{(0)}(\mathbf{x}) = \sum_{\rho>0} i_\rho^{(0)}(\mathbf{x}) W_\rho(\mathbf{x})$ are the lowest-order deterministic drift and work rate, respectively [28]. These are defined in terms of the detailed balanced deterministic currents $i_\rho^{(0)}(\mathbf{x}) = \omega_\rho^{(0)}(\mathbf{x}) - \omega_{-\rho}^{(0)}(\mathbf{x})$ constructed from the scaled transition rates evaluated at $W_\rho(\mathbf{x}) = 0$ that, according to the LDB conditions of Eq. (15), satisfy $\log(\omega_\rho^{(0)}(\mathbf{x})/\omega_{-\rho}^{(0)}(\mathbf{x})) = -\beta \Delta_\rho \cdot \nabla \phi(\mathbf{x})$. Comparing the result of Eq. (23) with Eq. (22), we see that $\dot{\Sigma}_a = 0$ to linear order in $W_\rho(\mathbf{x})$. As a consequence, to the same

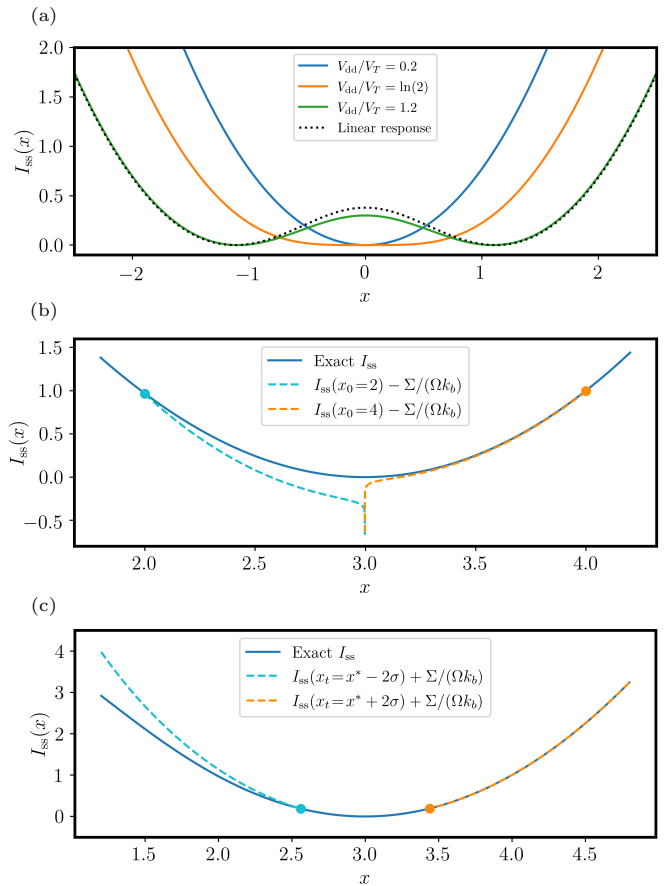


FIG. 1: (a) Rate function $I_{\text{ss}}(x)$ for different values of the powering voltage V_{dd} . We also compare $I_{\text{ss}}(x)$ with the linear response approximation obtained from Eq. (24) for $V_{\text{dd}} = 1.2V_T$. (b) Illustration of the bound to $I(x_t)$ in Eq. (3) for two different deterministic trajectories starting at $x_0 = 2$ and $x_0 = 4$ ($V_{\text{dd}} = 3V_T$). (c) Bound to $I(x_0)$ for a fixed x_t according to Eq. (3), for $x_t = x^* \pm 2\sigma$ ($\sigma = 1/\sqrt{2\Omega}$, $\Omega = 10$, and $V_{\text{dd}} = 3V_T$).

order, the equality is valid in Eq. (3). Then, in the linear response regime we can write:

$$\begin{aligned} \mathcal{I}(\mathbf{x}_t) - \mathcal{I}(\mathbf{x}_0) &\simeq -\Sigma^{(0)}/k_b \\ &= \beta \Omega \left[\phi(\mathbf{x}_t) - \phi(\mathbf{x}_0) - \int_0^t dt' \dot{w}^{(0)}(\mathbf{x}_{t'}) \right]. \end{aligned} \quad (24)$$

where the integration is performed along trajectories solving the detailed balanced deterministic dynamics $d_t \mathbf{x}_t = \mathbf{u}^{(0)}(\mathbf{x}_t)$.

IV. EXAMPLE

In order to illustrate our results we will consider the model of a low-power CMOS memory cell developed in [29, 30], that we review in the Supplementary Material. This model involves two CMOS inverters connected in a

loop, and each inverter is composed of two MOS transistors. There are two degrees of freedom: voltages v_1 and v_2 , that can take values spaced by the elementary voltage $v_e = q_e/C$, where q_e is the positive electron charge and C is a value of capacitance that increases with the scale of the MOS transistors. Thus, in this context the scale parameter can be taken to be $\Omega = V_T/v_e$, where $V_T = k_b T/q_e$ is the thermal voltage. The logical state of the memory is codified in the sign of the variable $x = (v_1 - v_2)/V_T$, and the rate function $I_{ss}(x)$ associated to the steady state distribution for x can be computed exactly:

$$I_{ss}(x) = x^2 + 2x \frac{V_{dd}}{V_T} + \frac{2n}{n+2} [L(x, V_{dd}) - L(x, -V_{dd})], \quad (25)$$

where V_{dd} is the powering voltage that takes the memory out of thermal equilibrium, $L(x, V_{dd}) = \text{Li}_2(-\exp(V_{dd}/V_T + x(1 + 2/n)))$, and $\text{Li}_2(\cdot)$ is the polylogarithm function of second order. Also, $n \geq 1$ is a parameter that characterizes the transistors (the slope factor).

In Figure 1-(a) we show that there is a non-equilibrium transition from a monostable phase into the bistable phase that allows the storage of a bit of information, occurring at the critical powering voltage $V_{dd}^* = \ln(2)V_T$ for $n = 1$. We also compare the exact rate function in Eq. (25) with the linear response approximation obtained from Eq. (24) for a powering voltage $V_{dd} = 1.2V_T$, well into the bistable phase. Remarkably, despite it is only expected to be valid close to equilibrium, the linear response approximation captures the transition to bistability. In Figure 1-(b) the exact rate function $I_{ss}(x_t)$ along a deterministic trajectory x_t is compared with the lower bound $I_{ss}(x_0) - \Sigma(t)/(\Omega k_b)$, for two different trajectories starting at $x_0 = 2$ and $x_0 = 4$. In both cases the trajectory x_t approaches the fixed point $x^* \simeq V_{dd}/V_T = 3$. We see that $I_{ss}(x_0) - \Sigma(t)/(\Omega k_b)$ is indeed a lower bound to $I_{ss}(x_t)$, in accordance with Eq. (3). Note that this bound diverges when the trajectory approaches the fixed point x^* . The reason is that once $x_t \simeq x^*$, the entropy production $\Sigma = -(\Omega/T) \int_0^t \dot{q}(x'_t) dt'$ just continuously integrates the steady state heat dissipation rate $-\dot{q}(x^*)$ (for this kind of circuits the internal electronic entropy can be neglected and therefore the entropy production Σ matches the entropy flow Σ_e). The linear response approximation avoids this issue since the lowest-order work rate $\dot{w}^{(0)}(x)$ vanishes at the equilibrium fixed point (see Eq. (24)). Alternatively, Eq. (3) can be considered an upper bound to $I(x_0)$ for a fixed final point x_t . This is shown in Figure 1-(c), for final points $x_t = x^* \pm 2\sigma$, where $\sigma = 1/\sqrt{2\Omega}$ estimates the variance of the fluctuations around the fixed point.

The fact that in Figures 1-(b, c) the bounds are much tighter to one side of the fixed point than the other can be traced back to the different speeds at which the fixed point is approached. To show this, in Figure 2 we have plotted the entropy production rate $\dot{\Sigma}$ and the speed

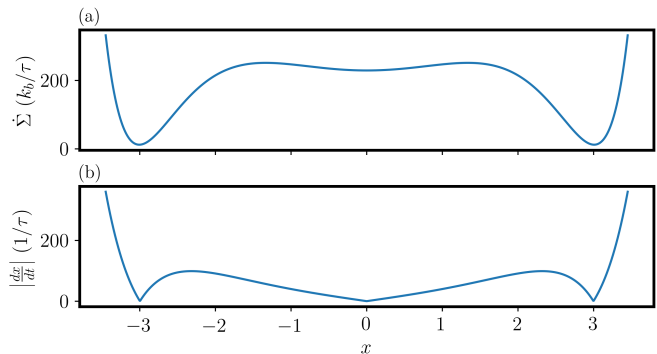


FIG. 2: (a) Deterministic entropy production rate $\dot{\Sigma}$, and (b) deterministic speed $|dx/dt|$ as a function of x for $V_{dd} = 3V_T$ (see the Supplementary Material for the definition of the timescale τ).

$|dx/dt|$ as a function of x for $V_{dd} = 3V_T$. In figure 2-(a) we see that $\dot{\Sigma}$ is minimized close to the deterministic fixed points (this is a design feature of CMOS devices, in order to minimize the static power consumption, which is however not zero). Also, we see that $\dot{\Sigma}$ is actually lower to the left of the fixed point at $x \simeq 3$ than to the right. However, in Figure 2-(b) we see that the speed dx/dt at which the fixed point is approached is also lower to the left side, resulting in a larger total entropy production $\Sigma = \int_0^t \dot{\Sigma}(x_t) dt = \int_{x_0}^{x_t} \dot{\Sigma}(x_t)/(dx/dt) dx$, and a looser bound in Figures 1-(b, c).

V. DISCUSSION

For systems accepting a description in terms of Markov jump processes, our results unveil a fundamental connection between the deterministic dynamics that emerges in a macroscopic limit and the non-equilibrium fluctuations at steady state. This is given by an inequality that can be interpreted as an emergent second law. In fact, it is a tighter version of the usual second law, that is saturated in the linear response regime. The practical value of our result lies in the fact that the probability of non-equilibrium fluctuations is hard to evaluate, while the deterministic dynamics is directly given by standard methods. In addition, the corresponding linear response theory, working at the level of the rate function, was shown in [28] to be highly accurate in some model systems, with a regime of validity beyond that of usual linear response theories. Our result can also be employed in combination with numerical approaches: once normal or moderately rare fluctuations have been numerically sampled and characterized, Eq. (3) can be used to bound the probability of very rare fluctuations, that otherwise would require extremely long simulation times.

VI. ACKNOWLEDGMENTS

We acknowledge funding from the INTER project “TheCirco” (INTER/FNRS/20/15074473) and CORE

project “NTEC” (C19/MS/13664907), funded by the Fonds National de la Recherche (FNR, Luxembourg), and from the European Research Council, project NanoThermo (ERC-2015-CoG Agreement No. 681456).

-
- [1] Sheldon Goldstein, Joel L Lebowitz, Roderich Tumulka, and Nino Zanghì. Canonical typicality. *Physical review letters*, 96(5):050403, 2006.
- [2] Sandu Popescu, Anthony J Short, and Andreas Winter. Entanglement and the foundations of statistical mechanics. *Nature Physics*, 2(11):754–758, 2006.
- [3] Hans-Otto Georgii. *Gibbs Measures and Phase Transitions*. De Gruyter, Berlin, Germany, May 2011.
- [4] Udo Seifert. Entropy production along a stochastic trajectory and an integral fluctuation theorem. *Physical review letters*, 95(4):040602, 2005.
- [5] Joel L Lebowitz and Peter G Bergmann. Irreversible gibbsian ensembles. *Annals of Physics*, 1(1):1–23, 1957.
- [6] JL Lebowitz. Stationary nonequilibrium gibbsian ensembles. *Physical Review*, 114(5):1192, 1959.
- [7] James A McLennan Jr. Statistical mechanics of the steady state. *Physical review*, 115(6):1405, 1959.
- [8] Dmitrii Nikolaevich Zubarev. *Nonequilibrium statistical thermodynamics*. Consultants Bureau, 1974.
- [9] DN Zubarev. Nonequilibrium statistical operator as a generalization of gibbs distribution for nonequilibrium case. *Cond. Matt. Phys*, 4(7), 1994.
- [10] Teruhisa S Komatsu and Naoko Nakagawa. Expression for the stationary distribution in nonequilibrium steady states. *Physical review letters*, 100(3):030601, 2008.
- [11] Christian Maes and Karel Netočný. Rigorous meaning of mclennan ensembles. *Journal of mathematical physics*, 51(1):015219, 2010.
- [12] Matteo Colangeli, Christian Maes, and Bram Wynants. A meaningful expansion around detailed balance. *Journal of Physics A: Mathematical and Theoretical*, 44(9):095001, 2011.
- [13] Abhishek Dhar, Keiji Saito, and Peter Hänggi. Nonequilibrium density-matrix description of steady-state quantum transport. *Physical Review E*, 85(1):011126, 2012.
- [14] H Ness. Nonequilibrium density matrix for quantum transport: Hershfield approach as a mclennan-zubarev form of the statistical operator. *Physical Review E*, 88(2):022121, 2013.
- [15] Hu Gang. Lyapounov function and stationary probability distributions. *Zeitschrift für Physik B Condensed Matter*, 65(1):103–106, 1986.
- [16] Riccardo Rao and Massimiliano Esposito. Conservation laws shape dissipation. *New Journal of Physics*, 20(2):023007, feb 2018.
- [17] Christian Maes. Local detailed balance. *SciPost Phys. Lect. Notes*, 32:1–17, 2021.
- [18] Jürgen Schnakenberg. Network theory of microscopic and macroscopic behavior of master equation systems. *Reviews of Modern physics*, 48(4):571, 1976.
- [19] Takahiro Hatano and Shin-ichi Sasa. Steady-state thermodynamics of langevin systems. *Physical review letters*, 86(16):3463, 2001.
- [20] Thomas Speck and Udo Seifert. Integral fluctuation theorem for the housekeeping heat. *Journal of Physics A: Mathematical and General*, 38(34):L581, 2005.
- [21] Massimiliano Esposito, Upendra Harbola, and Shaul Mukamel. Entropy fluctuation theorems in driven open systems: Application to electron counting statistics. *Phys. Rev. E*, 76(3):031132, Sep 2007.
- [22] Massimiliano Esposito and Christian Van den Broeck. Three faces of the second law. I. Master equation formulation. *Phys. Rev. E*, 82(1):011143, Jul 2010.
- [23] Hao Ge and Hong Qian. Physical origins of entropy production, free energy dissipation, and their mathematical representations. *Phys. Rev. E*, 81(5):051133, May 2010.
- [24] Riccardo Rao and Massimiliano Esposito. Detailed fluctuation theorems: A unifying perspective. *Entropy*, 20(9):635, 2018.
- [25] Hao Ge and Hong Qian. Mesoscopic kinetic basis of macroscopic chemical thermodynamics: A mathematical theory. *Physical Review E*, 94(5):052150, 2016.
- [26] Hugo Touchette. The large deviation approach to statistical mechanics. *Physics Reports*, 478(1-3):1–69, 2009.
- [27] Hugo Touchette and Rosemary J. Harris. Large deviation approach to nonequilibrium systems. *arXiv*, Oct 2011.
- [28] Nahuel Freitas, Gianmaria Falasco, and Massimiliano Esposito. Linear response in large deviations theory: A method to compute non-equilibrium distributions. *New J. Phys.*, Aug 2021.
- [29] Nahuel Freitas, Jean-Charles Delvenne, and Massimiliano Esposito. Stochastic Thermodynamics of Non-Linear Electronic Circuits: A Realistic Framework for Computing around kT. *arXiv (Accepted in PRX)*, Aug 2020.
- [30] Nahuel Freitas, Karel Proesmans, and Massimiliano Esposito. Reliability and entropy production in non-equilibrium electronic memories. *arXiv*, Mar 2021.

Supplementary material for “Emergent second law for non-equilibrium steady states”

Nahuel Freitas¹ and Massimiliano Esposito¹

¹*Complex Systems and Statistical Mechanics, Department of Physics and Materials Science, University of Luxembourg, L-1511 Luxembourg, Luxembourg*

PACS numbers:

Basic model – We provide here the details of the example given in the main text, based on the model of a non-equilibrium electronic memory developed in [1, 2]. This is a stochastic model of a low-power complementary metal-oxide semiconductor (CMOS) memory cell, whose circuit diagram is shown in Figure 1-(a). This circuit involves two identical CMOS inverters, or NOT gates, connected in a loop. Each inverter is in turn composed of a nMOS transistor and a pMOS transistor. The circuit is subjected to a voltage bias $2V_{dd}$, and it has two degrees of freedom: the voltages v_1 and v_2 at the output of each inverter. The total electrostatic energy of the full circuit is $\Phi(v_1, v_2) = (C/2)(v_1^2 + v_2^2) + CV_{dd}^2$, where C is a value of capacitance characterizing the circuit. The internal electronic entropy $S(v_1, v_2)$ is usually neglected in this kind of circuits, and therefore the entropy production is given by the entropy flow alone: $\Sigma = \Sigma_e = -Q/T$, where $-Q$ is the heat dissipated by the circuit.

Each transistor is modelled as a controlled conduction channel (see details in [1]), and two Poisson rates are associated to conduction events in forward and backward directions. In each conduction event, the voltages $v_{1/2}$ can change by the elementary voltage $v_e = q_e/C$. The Poisson rates can be derived from the I-V curve characterization of the transistors and the local detailed balance conditions [1]. For example, for the pMOS transistor in the first inverter one obtains the following Poisson rates (in subthreshold operation):

$$\begin{aligned} \lambda_+^p(v_1, v_2) &= (I_0/q_e) e^{(V_{dd}-v_2-V_{th})/(nV_T)} \\ \lambda_-^p(v_1, v_2) &= \lambda_+^p(v_1, v_2) e^{-(V_{dd}-v_1)/V_T} e^{-(v_e/2)/V_T}, \end{aligned} \quad (1)$$

In the previous equations, $V_T = k_b T/q_e$ is the thermal voltage and I_0 , V_{th} , and n are parameters characterizing the transistor (respectively known as *specific current*, *threshold voltage*, and *slope factor*). Assuming those parameters are the same for all the transistors, the Poisson rates associated to the nMOS transistor in the first inverter are just $\lambda_{\pm}^n(v_1, v_2) = \lambda_{\pm}^p(-v_1, -v_2)$, while the Poisson rates associated to the transistors in the second inverter are given by $\mu_{\pm}^{n/p}(v_1, v_2) = \lambda_{\pm}^{n/p}(v_2, v_1)$. The total rate for a transition $v_1 \rightarrow v_1 + v_e$ is $A(v_1, v_2) = \lambda_+^p(v_1, v_2) + \lambda_-^n(v_1, v_2)$, and the total rate for a transition $v_1 \rightarrow v_1 - v_e$ is $B(v_1, v_2) = \lambda_-^p(v_1, v_2) + \lambda_+^n(v_1, v_2)$. Then, the state of the system is

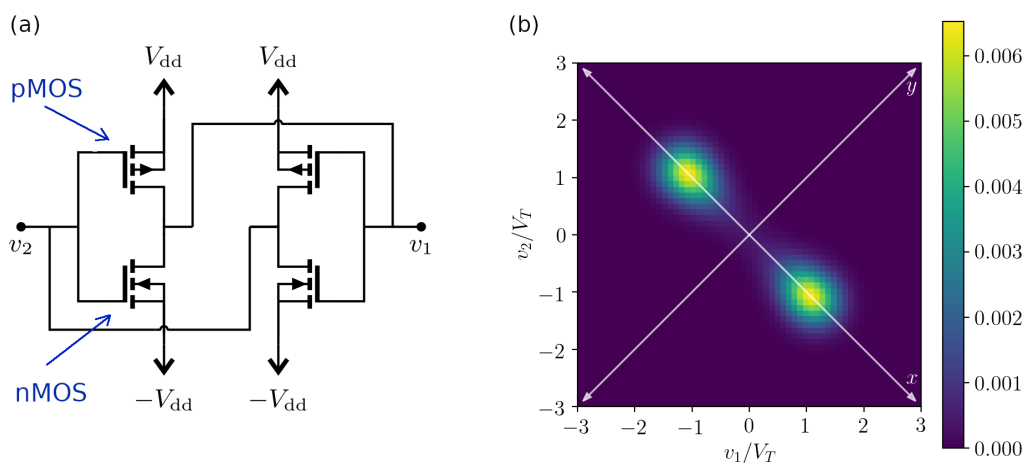


FIG. 1: (a) CMOS implementation of a bistable logical circuit involving two NOT gates in a loop, where each NOT gate is constructed with one pMOS (top) and one nMOS (bottom) transistors. This is the usual way SRAM memory cells are implemented. (b) 2D histogram of the steady state distribution ($V_T = 26$ mV, $v_e/V_T = 0.1$, $V_{dd}/V_T = 1.2$).

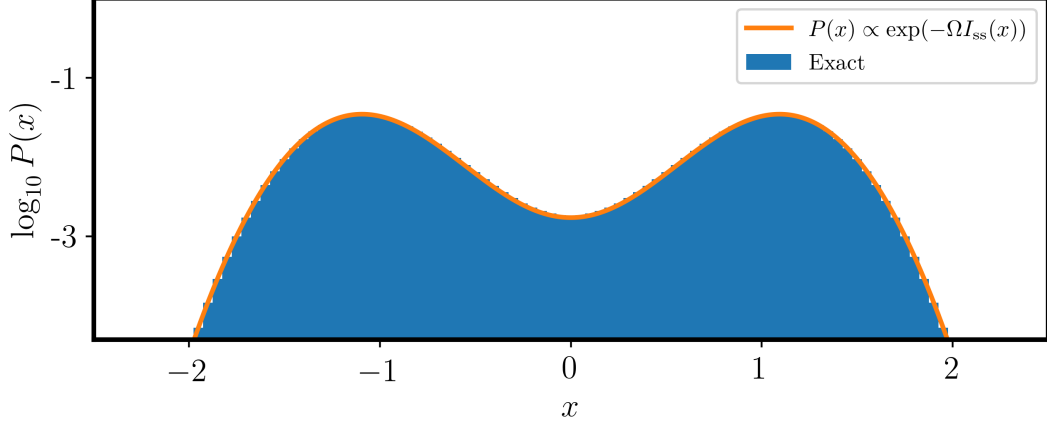


FIG. 2: Comparison between the exact steady state distribution for x and the LD approximation obtained from the rate function $I_{ss}(x)$ in the main text. ($\Omega = 10$ and $V_{dd} = 1.2V_T$).

described by a probability distribution $P(v_1, v_2, t)$ that evolves according to the master equation

$$d_t P(v_1, v_2, t) = PA|_{v_1-v_e, v_2} + PB|_{v_1+v_e, v_2} + PA^*|_{v_1, v_2-v_e} + PB^*|_{v_1, v_2+v_e} - P(A + B + A^* + B^*)|_{v_1, v_2}, \quad (2)$$

where we are using the compact notation $PA|_{v_1, v_2} = P(v_1, v_2, t)A(v_1, v_2)$, and $A^*(v_1, v_2) = A(v_2, v_1)$. One can numerically compute the steady state distribution from the previous master equation by truncating the state space to a finite number of dimensions. An example is shown in Figure 1-(b).

Macroscopic limit – A macroscopic limit can be introduced by considering a particular scaling of the physical dimensions of the transistors. In a MOS transistor there are two characteristic dimensions defined with respect to the conduction channel [3]: the length L and the width W . For fixed L , both the capacitance C and the characteristic current I_0 increase linearly with W . Thus, we can consider $\Omega = V_T/v_e \propto W$ as the adimensional scale parameter in the main text. In the following we consider the adimensional voltages v_1 and v_2 , in units of V_T . We also define the scaled rates $a(v_1, v_2) = \lim_{\Omega \rightarrow +\infty} A(v_1, v_2)/\Omega$ and $b(v_1, v_2) = \lim_{\Omega \rightarrow +\infty} B(v_1, v_2)/\Omega$. Then, introducing the large deviations ansatz $P_{ss}(v_1, v_2) \propto \exp(-v_e^{-1}I_{ss}(v_1, v_2))$ in the master equation and keeping only the dominant terms in v_e^{-1} , we obtain the following differential equation for $I_{ss}(v_1, v_2)$:

$$0 = (e^{\partial_{v_1} I_{ss}} - 1) a(v_1, v_2) + (e^{-\partial_{v_1} I_{ss}} - 1) b(v_1, v_2) + (e^{\partial_{v_2} I_{ss}} - 1) a(v_2, v_1) + (e^{-\partial_{v_2} I_{ss}} - 1) b(v_2, v_1). \quad (3)$$

As shown in [2], evaluating the previous equation at $y = v_1 + v_2 = 0$ leads to a differential equation for the reduced rate function $I_{ss}(x)$ associated to the variable $x = v_1 - v_2$ (this is justified by the contraction principle and the fact that the most probable value of y for any value of x is $y = 0$, see Figure 1-(b)). In that way it is possible to derive the expression for $I_{ss}(x)$ given in the main text. In Figure , we compare the probability distribution corresponding to that analytical rate function with exact numerical results. The agreement is essentially perfect even if only a few tens of electrons are involved (the scaling parameter is $\Omega = 10$, and $V_{dd} = 1.2V_T$).

Deterministic dynamics – The deterministic equations of motion for the circuit in Figure 1-(a) read:

$$\begin{aligned} CV_T d_t v_1 &= a(v_1, v_2) - b(v_1, v_2) = i(v_1, v_2) - i(-v_1, -v_2) \\ CV_T d_t v_2 &= a(v_2, v_1) - b(v_2, v_1) = i(v_2, v_1) - i(-v_2, -v_1), \end{aligned} \quad (4)$$

where $i(v_1, v_2) = I_0 e^{(V_{dd}/V_T - V_{th}/V_T - v_2)/n} (1 - e^{-(V_{dd}/V_T - v_1)})$ is the deterministic electric current through the pMOS transistor for given v_1 and v_2 . Alternatively, in terms of variables x and y defined above,

$$\begin{aligned} CV_T d_t x &= i(x, y) - i(-x, -y) - i(-x, y) + i(x, -y) \\ CV_T d_t y &= i(x, y) - i(-x, -y) + i(-x, y) - i(x, -y), \end{aligned} \quad (5)$$

where the change of variables in the functions $a(.,.)$ and $b(.,.)$ is implicit. Noting that $d_t y|_{y=0} = 0$ for all x , we realize that $y(t) = 0$ for all t if we have $y(0) = 0$. This is the case for the deterministic trajectories used to produce Figure 1-(c) in the main text. Finally, we note that the total deterministic work rate for given values of voltages v_1 and v_2 is

$\dot{W} = V_{\text{dd}}[i(v_1, v_2) + i(-v_1, -v_2) + i(v_2, v_1) + i(-v_2, -v_1)]$. The scaled work rate defined in the main text is in this case $\dot{w} = \dot{W}v_e/V_T$. The detailed balance drift $\mathbf{u}^{(0)}$ and the lowest order work rate $\dot{w}^{(0)}$ are obtained from the previous expressions by evaluating the currents $i(v_1, v_2)$ at $V_{\text{dd}} = 0$. Note also that the deterministic dynamics has a natural timescale $\tau = CV_T/(I_0 e^{-V_{\text{th}}/nV_T})$.

-
- [1] Nahuel Freitas, Jean-Charles Delvenne, and Massimiliano Esposito. Stochastic Thermodynamics of Nonlinear Electronic Circuits: A Realistic Framework for Computing Around kT . *Phys. Rev. X*, 11(3):031064, Sep 2021.
- [2] Nahuel Freitas, Karel Proesmans, and Massimiliano Esposito. Reliability and entropy production in non-equilibrium electronic memories. *arXiv*, Mar 2021.
- [3] Yannis Tsididis and Colin McAndrew. *Operation and Modeling of the MOS Transistor*. Oxford Univ. Press, 2011.

